

# **AFCI Quarterly Input – UNLV**

## **October through December, 2003**

### **1.0 University of Nevada, Las Vegas (UNLV)**

**UNLV Transmutation Research Program.** The University of Nevada, Las Vegas supports the AFCI through research and development of technologies for economic and environmentally sound refinement of spent nuclear fuel. The UNLV program has four components: infrastructure, international collaboration, student-based research, and management and program support.

#### **1.1 Infrastructure Augmentation**

##### ***1.1.1 Infrastructure Augmentation Scope***

The infrastructure augmentation component of the UNLV Transmutation Research Program enhances UNLV's research staff, facilities, and academic programs to increase the ability of the university to perform AFCI research.

##### ***1.1.2 Infrastructure Augmentation Highlights***

- **Ph.D. Program in Radiochemistry.** The proposal for a new Ph.D. program in Radiochemistry was submitted to the Board of Regents of the University and Community College System of Nevada at the end of December. The Board should address the proposal next quarter. If approved, the program could start as early as fall term 2004. The program will be a joint program between the Department of Chemistry and the Department of Health Physics and will be governed by the Graduate College.
- **Facilities Progress Update.** Drs. Sviatoslav Ignatiev and Olga Reshetnikova (IPPE, Russia) visited UNLV to begin the installation phase of the ISTC TC-1 lead bismuth target. The primary purpose of this trip was to determine the work that will be required to begin operation of the TC-1 at UNLV. This work is expected to be completed by March 2005. The Transmission Electron Microscope was installed this quarter. Next quarter a magnetic and acoustic interference shielding will be installed. Two other facilities, the Inductively Coupled Plasma Atomic Emission Spectrometer user facility and an interim Actinide Chemistry laboratory are progressing slower than expected and are still in the design phase for the ventilation system. The ICP AES and actinide chemistry equipment have arrived at UNLV and are awaiting installation, but additional ventilation is required in the rooms. The remodeling should be completed within the next two quarters.

#### **1.2 International Collaboration**

##### ***1.2.1 International Collaboration Scope***

The international collaboration component of the UNLV Transmutation Research Program enhances UNLV's breadth of scientific and scholastic experience. University collaboration is also an efficient conduit for international collaboration that benefits the national AFCI program. UNLV has ongoing relationships with the Khlopin Radium Institute (KRI) in St. Petersburg, Russia; the Institute for Physics and Power Engineering (IPPE) in Obninsk, Russia; and members

of the International Molten Metal Advisory Committee (from Sweden, Germany, Belgium, and Italy).

### ***1.2.2 International Collaboration Highlights***

- **International Science and Technology Center (ISTC).** Two Russian scientists visited UNLV to start the installation of the ISTC Target Complex 1. Complete installation is expected in March 2005.
- **Khlopin Radium Institute.** Dr. Boris Burakov (KRI, Russia) visited UNLV for collaboration meetings on Tasks 15 and 16 and to discuss future collaborations and technology transfers regarding actinide containing ceramic fabrication and analysis.

## **1.3 Student Research**

### ***1.3.1 Student Research Scope***

The Student Research component is the core of the UNLV Transmutation Research Program with steadily increasing funds as the program evolves and capability expands. The milestones, schedules, and deliverables of the student research projects are detailed in the individual research proposals. UNLV currently has 16 student research tasks that include 37 graduate students and involve 28 faculty members. The tasks are divided below in terms of their research area: fuels, separations, and transmutation sciences.

### ***1.3.2 Student Research Highlights***

#### **FUELS TECHNOLOGY**

##### **Metallic Fuel Pins (Task 1) Highlights.**

- A model was developed to determine the power deposition rate (Q) for the induction heating system based on two complex component values of C and S for the induction current. Model results agree with theoretical analysis and experiments.
- Comparisons of the induction heating process for the different current frequencies have been studied. We find that a relatively high current frequency is needed to melt the feedstock. If the frequency is not high enough, the temperature will take too long (if ever) to reach the melting point of the feedstock material because the heat sink will absorb the deposited power very quickly.
- Comparisons of the induction heating process for different current densities have been studied. We find that a high current density will increase the temperature very quickly. The current density has a greater impact on the induction heating system than the current frequency. Also, we doubled the current density and found that the time of heating the feedstock to melting point was shortened from 360 seconds to about 18 seconds. The maximum temperature reaches to 2000 °C in 0.5 seconds if we use a higher current density. From this analysis we may conclude that the current density is the key to adjust the power deposition and the heat efficiency.
- The 2-D and 3-D plots of the time average power deposition  $Q$  ( $\text{w/m}^3$ ) output agree with the theoretical analysis that the maximum value of time average power deposition lies in the “skin” and the top of the feedstock.
- The value of the time average power deposition (Q) decreases quickly and approaches zero near the center of the metal feedstock. (“Skin effect”)

- We have also found that the feedstock is heated up quickly and then is melted. Since the induction heating has very high efficiency, the maximum temperature can be reached within a very short time. Although the maximum temperature has been reached at an incredible speed, the melt region is developed at a reasonable speed toward the center of the feedstock during the continuous heat transfer process.

### **Remote Fuel Fabrication (Task 9) Highlights.**

- Hot cell robotic assembly and pick and place dynamic simulations, including feedback control with Matlab, were performed.
- Jae-Kyu Lee passed the Ph.D. final examination. Mr. Lee submitted the completed thesis, including the modifications required by the committee, to the Graduate College. Thesis title: “Three Dimensional Pattern Recognition using Feature-Based Indexing and Rule-Based Search.”

## **SEPARATIONS TECHNOLOGY**

### **Systems Engineering Model (Task 8) Highlights.**

- Due to the sensitivity restrictions on the AMUSE code, the system model has considered and assumed that AMUSE is treated as a black box during the optimization.
- A middleware-like module, Flowsheet Simulator, was designed to accommodate the integration restriction of extraction processes, such as UREX, Pu/Np, Cs/Sr or MA process.
- Currently the Flowsheet Simulator will identify the input parameters provided from the UREX process or AMUSE code, and it will generate required data formats and a database for the system engineering model.
- The detailed system engineering model was developed to provide numerous functions for system analysis. Each block is an independent module that can be integrated into the system.
- Mr. Lijian Sun successfully defended his thesis for Master of Science degree on November 14. Thesis title: “Development of a Systems Engineering Model for Chemical Separation Process.”
- Work continued on the User interface, focusing primarily on the graph page dialog. Additional features, including the ability to customize display and output formats, were added to the interface.
- The Rosenbrock function was used as a test problem to optimize algorithms. It is also called the banana function because of the way the curvature bends around the origin as shown in the following figure. It is notorious in optimization examples because of the slow convergence which most methods exhibit when trying to solve this problem. We model this problem by way of Calculation model. The optimization techniques adopted were both the Conjugate Gradient method and the Random Walk method.
- The interface was completed but will need some verifiable data sets for testing runs.

### **Criticality and Heat Transfer Analyses of Separations Processes (Task 11) Highlights.**

- Completion of Masters Thesis and Defense by Elizabeth Bakker on November 14. Thesis title: “Criticality and Thermal Analysis of Separated Actinides in Transmutation.”
- Completion of report on cesium/strontium storage forms to be submitted as published document.

### **Immobilization of Fission Iodine (Task 15) Highlights.**

- Continued to investigate the formation of volatile iodides in aqueous suspensions of NOM with iodine. We performed some experiments on recovery of iodide from the fuel rod simulator.
- Continued to examine the speciation of iodine remaining in water soluble forms after reaction of active iodine with NOM.
- Continued to investigate and quantify the release of methyl iodide from iodine treated NOM.
- Continued to investigate the reactivity of a mercaptan group (-SH) a selenol (SeH) containing resin for methyl iodide trapping.
- Performed some additional experiments on measuring iodine reaction kinetics with NOM in aqueous suspensions.
- Continued experiments with FCC and NOM scavenging of iodine during simulated fuel dissolution. Explored the speciation of iodine on FCC and NOM. The formation of iodate as a result of exposure to NO<sub>x</sub> has been documented. Under some circumstances iodate forms extensively on the scavenging medium. There are distinct differences between the iodine generator and the fuel rod simulator.
- Continued additional elemental analysis (CSN) on KRI FCC material and NOM.
- We are revisiting pH dependence of the reaction of iodine with model compounds and with NOM. We are examining the reaction of iodine with vanillin and acetovanillone at various pHs. We have observed changes in product distributions with pH for the vanillin experiment.

### **Fluorapatite Waste Forms (Task 16) Highlights.**

- Obtained single crystal diffraction data for fluorapatite crystal.
- Worked on solid state synthesis of fluorapatite bearing Zn.
- Obtained TG/DSC for hydroxyapatite and hydroxyapatite with Zn cations.
- Obtained FTIR spectra for two samples (hydroxyapatite and Zn-containing hydroxyapatite) calcinated at 750 degrees centigrade.
- Obtained XPS spectra of the same two samples.
- Synthesis of two synthetic apatites completed:
  - Mixture One = Fluorapatite + Calcium Fluoride + ZnO
  - Mixture Two = Hydroxyl Apatite + Calcium Fluoride + ZnO
- Mixtures were heated to 1150 degrees in an oven for 3 hours and the resulted compounds were analyzed using Photo caustic IR. Results were compared with the IR spectra obtained for the mixtures (mixture before heating). Significant changes in IR spectra were observed (after heating and before heating).

- Synthesized compounds were washed in Nitric acid and dried in air in preparation of SEM Imaging. Results were inconclusive. Scheduled another session to use the SEM for further analysis.
- Synthesized Strontium-containing Fluorapatite by reflux method (at different concentrations of SrCl<sub>2</sub> for different refluxing time periods).
- Optimized conditions for this synthesis, i.e., refluxing times and best concentrations.
- Prepared two Zn containing hydroxyapatite samples using two different Zinc nitrate concentrations (using two different amounts of Zinc cations)
- Obtained SEM micro graphs and XPS spectra of the Zn-containing samples.

## TRANSMUTATION SCIENCES

### Niobium Cavity Fabrication Optimization (Task 2) Highlights.

- Manipulator designs to move test piece and to measure electron beam current were completed.
- *In situ* Ar cleaning and water removal system at 10<sup>-8</sup> Torr was designed and finalized.
- Secondary emission code was obtained from Dr. Joy from ORNL and University of Tennessee Knoxville.
- Multipacting code being used to study muffin tin cavity.
- Existing vacuum chamber port incompatible with cryostat positioning unit. Cost to modify port is as much as purchasing a compatible chamber. New chamber with ports aligned with center has been purchased. Systems being built. Delivery date before Christmas.
- LANL supplied us with surface conditioned Nb samples and raw Nb rod of the grade used in building their chambers.
- Monte Carlo Back Scattering and Secondary Electron Scattering code is being modified to account for surface layer contamination.
- M.S. thesis by S. Subramanian on flow studies was successfully defended. Theses title: “Modeling, Optimization, and Flow Visualization of Chemical Etching Process in Niobium Cavities.”

### LBE Corrosion of Steel (Task 3) Highlights.

- Sample prep techniques have been developed to preserve the surface layers for quantitative analysis of samples by electron microprobe. Analysis of samples is underway.
- Development of epoxy resin techniques to stabilize alteration layers for SEM/EMPA analysis continued.
- XPS methodologies to attempt to determine chemical states in the samples were investigated.

### Environment-induced Degradation of Materials (Task 4) Highlights:

- SCC tests using self-loaded C-ring and U-bend specimens were ongoing in aerated acidic solution at elevated temperatures. These test specimens are periodically withdrawn from the cells for verification of crack initiation by optical microscopy. The results indicate that the C-ring specimens of Alloy HT-9 showed through-thickness cracking in the acidic solution at 50 and 100°C. Cracking tendency was also observed in the U-bend specimens

of Alloys EP-823 and HT-9 in the acidic solution at 100°C. SCC testing in the molten LBE using similar types of specimens is in progress at LANL.

- Simultaneously, SCC testing using smooth and notched tensile specimens of Alloys EP-823, HT-9 and 422 are ongoing under constant load in the MPL.
- Fractographic evaluations by scanning electron microscopy are being continued. Microstructural analyses by optical microscopy are also in progress.

#### **LBE Corrosion Modeling (Task 5) Highlights:**

- Simulations of corrosion/precipitation flux in elbow geometries have been completed. Significant divergences from previous predictions have been observed in these simulations, indicating that previous analytical models were not sufficiently modeling the system behavior.
- Mr. Dasika's MS thesis has been completed and approved by the graduate college.
- A 3-D model for a sudden expansion has been developed. The model is currently being tested for grid independence.
- Work on 3-Dimensional computational fluid dynamics (CFD) models of pipe fittings continued.

#### **Dose Conversion Coefficients (Task 7) Highlights:**

- Dose coefficients are being calculated for Category 2 radionuclides.
- We had our semi-annual DC meeting to discuss the focus of the consortium.
- A plan was devised to calculate all DCs which have reported values.
- Work has begun on our second publication of dose coefficients.
- A subcontract was finalized for workers in the Republic of Georgia.

#### **Properties of Alloy EP-823 (Task 10) Highlights:**

- Mechanical testing of two different heats of Alloy EP-823 and one heat of Alloy HT-9 is ongoing at elevated temperatures in the presence of nitrogen using an MTS machine. Additional tensile specimens are being machined to study the effect of tempering times on the mechanical properties at different temperatures.
- Heat treatments of Type 422 stainless steel were completed.
- Metallography and fractography are in progress involving all tested tensile specimens.

#### **Oxygen Sensing in LBE (Task 13) Highlights:**

- FEMlab simulation of the transport phenomena for the oxygen calibration system continued.
- Simulation of the transport phenomena for the oxygen calibration system using self-written codes and FLUENT continued at UNLV.
- The first run of experiments on the Oxygen Sensor System were completed at LANL.
- Mr. R. Sivaraman successfully defended his M.S. thesis on Nov. 14.

#### **Positron Annihilation Spectroscopy (Task 14) Highlights:**

- Welded, cold-worked and bent specimens of Alloys EP-823 and HT-9, and Type 304L stainless steel have been tested at the Atomic Energy of Canada Limited (AECL) for residual stress measurements by neutron diffraction (ND) technique. Comparisons of the

ND data to those obtained by the ring-core method showed consistent results. A similar trend in the measured residual stresses was also observed between the ND and positron techniques.

- Residual stress measurements by the positron annihilation spectroscopy are ongoing on different types of specimens at the Idaho Accelerator Center of ISU.

### 1.3.3 Student Research Technical Summary

#### FUELS TECHNOLOGY

**Metallic Fuel Pins (Task 1).** The analysis of mold filling and solidification continues with progress being made for the consideration of these two features within one model. Analysis of the induction heating process of an Induction Skull Melter (ISM) is under study. Efforts are underway to validate the modeling procedure and specific comparisons are being made to previously published work. Few detailed modeling results have been reported by other researchers, making the validations an important part of the overall modeling process. Skin heating depths, power deposition rates, and other process parameters are being evaluated for use in upcoming furnace design simulations. Efforts are beginning on the development of a numerical model that assesses the impact of americium transport from a heated melt. Figure 1.3.1 shows the temperature contours of an induction furnace.

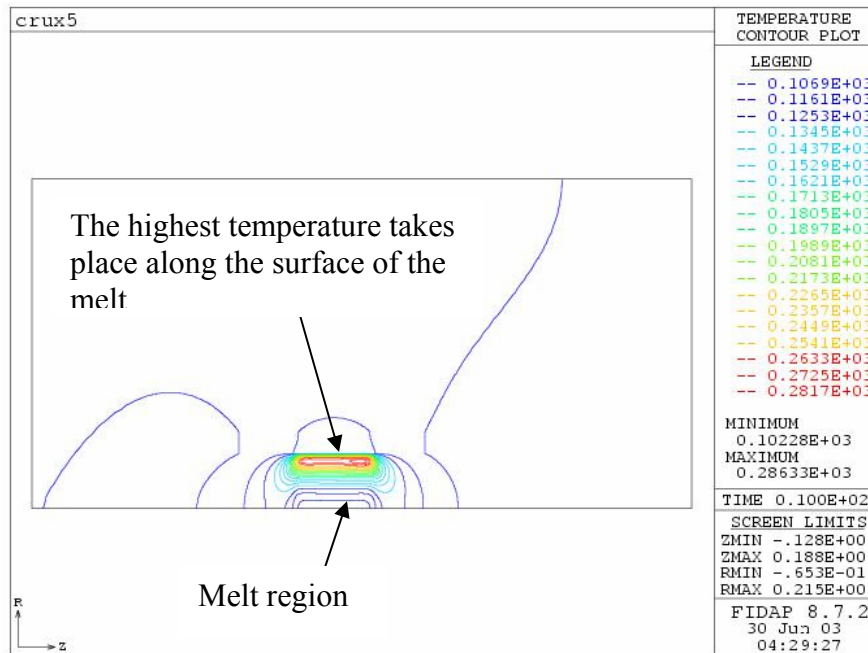


Figure 1.3.1. The temperature contours of induction heating furnace

The mold filling process and the solidification modeling have been combined and simulated together using the VOF-solidification algorithm. The solidification could take place during the filling process. Since the casting process is very difficult and complicated, the software FIDAP alone is not enough for this kind of numerical simulation. Thus, two FORTRAN subroutines have been developed to link with FIDAP in the calculation.

In the casting process, the velocity profiles are found increasing rapidly and then dropping off as solidification occurs. Figure 1.3.2 shows the velocity profiles for the different time steps in the VOF-solidification process. Average inlet velocity is 1 m/s. The parabolic velocity profile has been used. The mold material is copper. Inlet temperature is 1,500 °C. Heat transfer coefficient is 2,000 W/m<sup>2</sup>°C and mold preheated temperature is 800 °C.

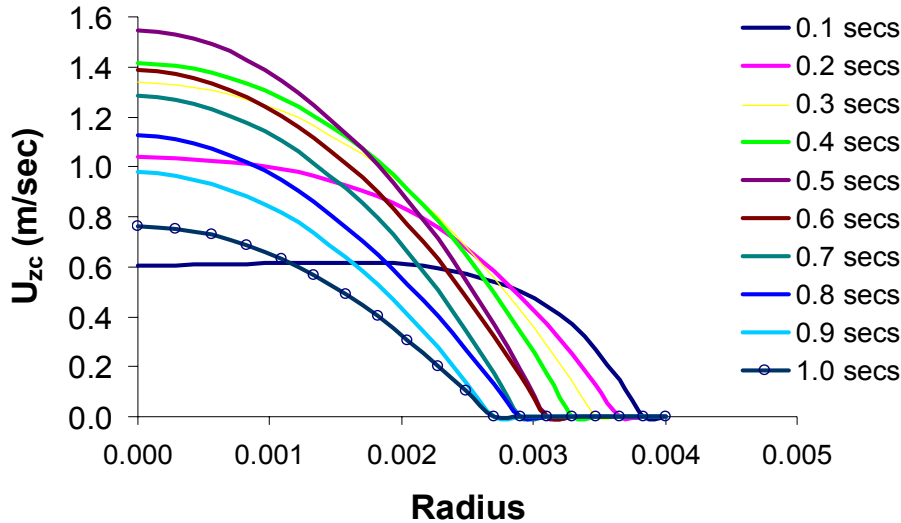


Figure 1.3.2. Axial velocity profile for constant inlet pressure of 20 kPa (mold preheated temperature=800 °C, inlet melt temperature=1,500 °C, interfacial heat transfer coefficient =2,000 W/m<sup>2</sup>°C).

A new system design using a plug at the end of the mold which can control the backward pressure inside the mold has been suggested by ANL-West. Hence, two fluids VOF method will be used to include air and melt during the casting process. Skin heating depths, power deposition rates, and other process parameters have been continuously evaluated for use in upcoming furnace design simulations.

Efforts are beginning on the development of a numerical model that assesses the impact of americium transport from a heated melt. The heating rates with temperature profiles with the different power deposition to the crucible have been studied.

We continue to work on the induction heating system of crucible modeling. The differences of the required heating time to reach the melting temperature by increasing the coil numbers have been studied.

Two different coil numbers n=5 and n=6 have been used. The heating time is about 450 seconds when n=5 and 200 seconds when n=6 to reach the melting temperature of 1,400 °C based on d=3 mm and b=10 mm. The dimensions of b and d are also the important factors in the induction heating system modeling. The modified design of d=2 mm, b=5 mm, and n=6 instead of d=3

mm,  $b=10$  mm, and  $n=5$  has been studied. The modified design of induction heating system shows about 3 times faster than the original design for temperature to reach the melting point  $1,400$  °C. Figure 1.3.3 shows the time requirement for reaching the melting point using the different coil numbers.

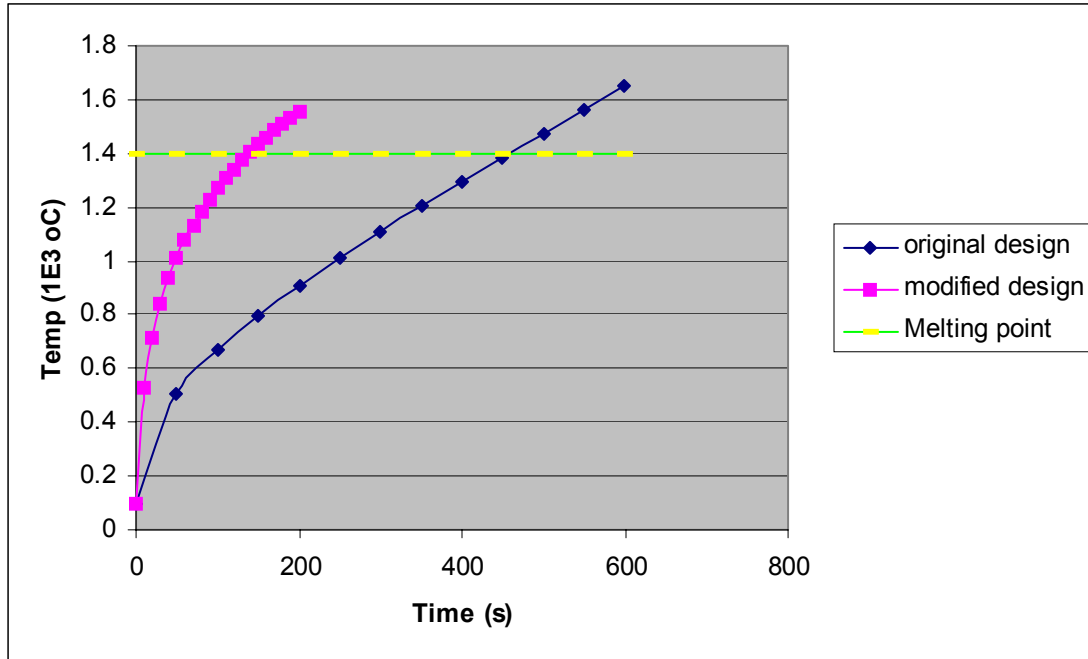


Figure 1.3.3. The time requirements for reaching the melting point using the different coil numbers.

As in most materials, especially in the oxides, the electrical conductivity is strongly dependent on temperature. From the former work we know electrical conductivity has great impact on the calculation of the two complex components of power deposition. A subroutine has been developed in the simulation of induction heating problem when the electrical conductivity is a variable value. From this subroutine we can use a loop to calculate the temperature distribution in the system.

It will be difficult to use low electrical conductivity materials on the induction heating system. It will be necessary to add a pure material such Zr which has the high electrical conductivity to  $ZrO_2$  powder. Zr acts as a “conductor” during the induction heating process. The location of the “conductor” material, shape, and volume are important factors during the numerical modeling. We have assumed the “conductor” material has a loop shape and we revised our computational domain.

### Remote Fuel Fabrication (Task 9).

Part I: Hot Cell Manipulator Simulation. During the present reporting period, the simulation model for the fuel manufacturing process was improved further by graduate student Jamil Renno. Matlab controls the spatial robot model, comprising a geometric model as well as the robot dynamics. Thus a realistic simulation of the forces and torques present during robot motion is

being generated. Jamil developed a simulation for pellet placement from a bin, and for inserting a row of pellets into a fuel rod. A 3-D simulation model of a partial hot cell manufacturing plant consisting of pellet press, sintering oven, inspection station, and cladding tube filling station was created as illustrated in Figure 1.3.4. Several accident scenarios associated with pellet placement and insertion were explored and analyzed. Fig. 1.3.5 presents an example of failed pellet insertion into the cladding tube.

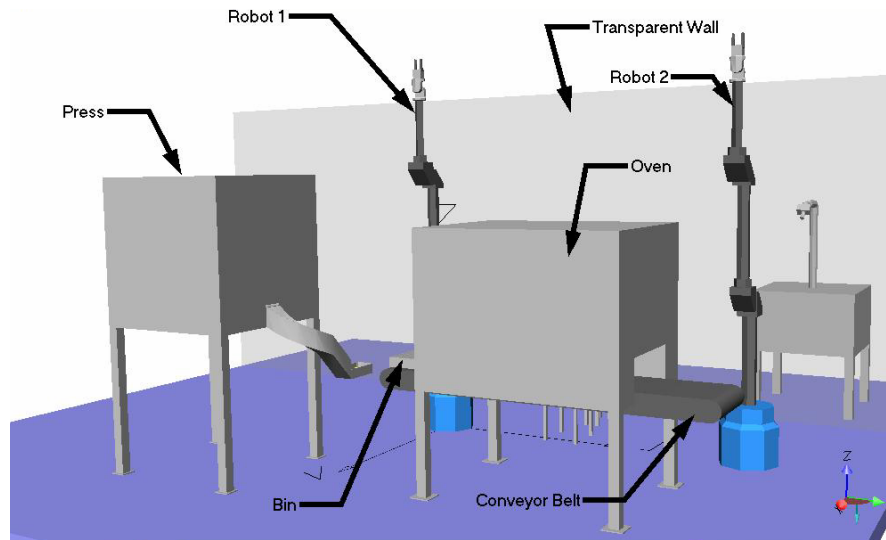


Figure 1.3.4. Robot Simulation: Hot Cell Manufacturing Plant Consisting of Pellet Press, Sintering Oven, Inspection Station, and Cladding Tube Filling Station.

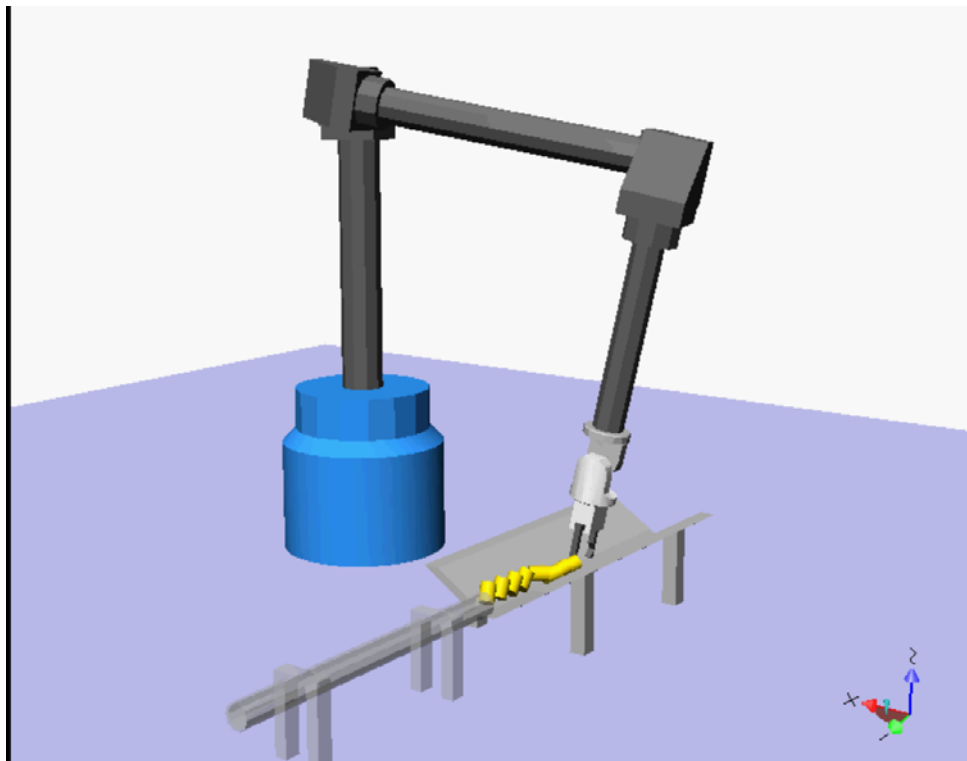


Figure 1.3.5. Pellets Buckling due to Excessive Pushing Force from the Robot.

Mr. Jae-Kyu Lee continued his work on recognition using a knowledge-based system. Mr. Lee completed the defense of his thesis in November 2003. A copy of the final Ph.D. document is transmitted separately.

Part II: Object Recognition. Jae-Kyu Lee continued his work on recognition using a knowledge-based system. Mr. Lee completed the defense of his Ph.D. thesis in November 2003 entitled “Three Dimensional Pattern Recognition using Feature-Based Indexing and Rule-Based Search.”

## SEPARATIONS TECHNOLOGY

**Systems Engineering Model (Task 8).** The objectives of this task are the development of a systems engineering model and the refinement of the Argonne code AMUSE (Argonne Model for Universal Solvent Extraction). The detailed systems engineering model is the start of an integrated approach to the analysis of the materials separations associated with the AFCI Program. A second portion of the project is to streamline and improve an integral part of the overall systems model, which is the software package AMUSE.

Efforts have started on the storage of all results in a MS-Access database to speedup and streamline the analysis of multiple runs (parametric studies for design purposes). An Object Oriented Programming (OOP) approach has been developed and implemented for the final three sections of the new modeling approach (First, Intermediate, and Last sections). A number of AMUSE analyses were conducted to demonstrate the ability of the code to store the data, plot the data, and to obtain feedback from ANL on how to improve the interface. The AMUSE code can now be called from within MATLAB as part of the Systems Engineering Modeling effort.

Input files and results files can be successfully generated for individual runs and for multiple runs through MATLAB calls. Refinements will be made to this approach to allow for more runs and to allow for optimization. We have successfully implemented the OOP. Move command is also implemented to the three sections. The database has been created and tested using ACCESS of Microsoft. SQL server has been used to implement the database design. Tables were modified completely so that redundancy is reduced. Four tables can take all the data from the VB interface. Tables have been designed for output so that reports can be generated from the developed interface by NCACM instead of AMUSE. Each table has filename as primary key so that foreign key relationship can be established. It enables user to easily handle the data for a particular flow sheet.

Several runs were made and charts for different inputs versus outputs were created. Based on these charts we have got some relationship between input and output which can be used for optimization process in the system engineering modeling.

FLOWSHEET-SIMULATOR has been developed which has the following features:

- Create a new FLOWSHEET from scratch
- Open a FLOWSHEET from export file
- Open a FLOWSHEET from SQL server database
- Edit the FLOWSHEET by simply visually dragging and dropping

- Save result to database
- Save result to export file
- Call AMUSE code to run

The great advantages of the FLOWSHEET-SIMULATOR are that it is developed using OOP technologies and can hide all the information about connection with AMUSE and data flow with database, export file and report file. FLOWSHEET-SIMULATOR provides the entire friendly interface for user to implement all the functions. A FLOWSHEET-SIMULATOR screen is shown in Figure 1.3.6.

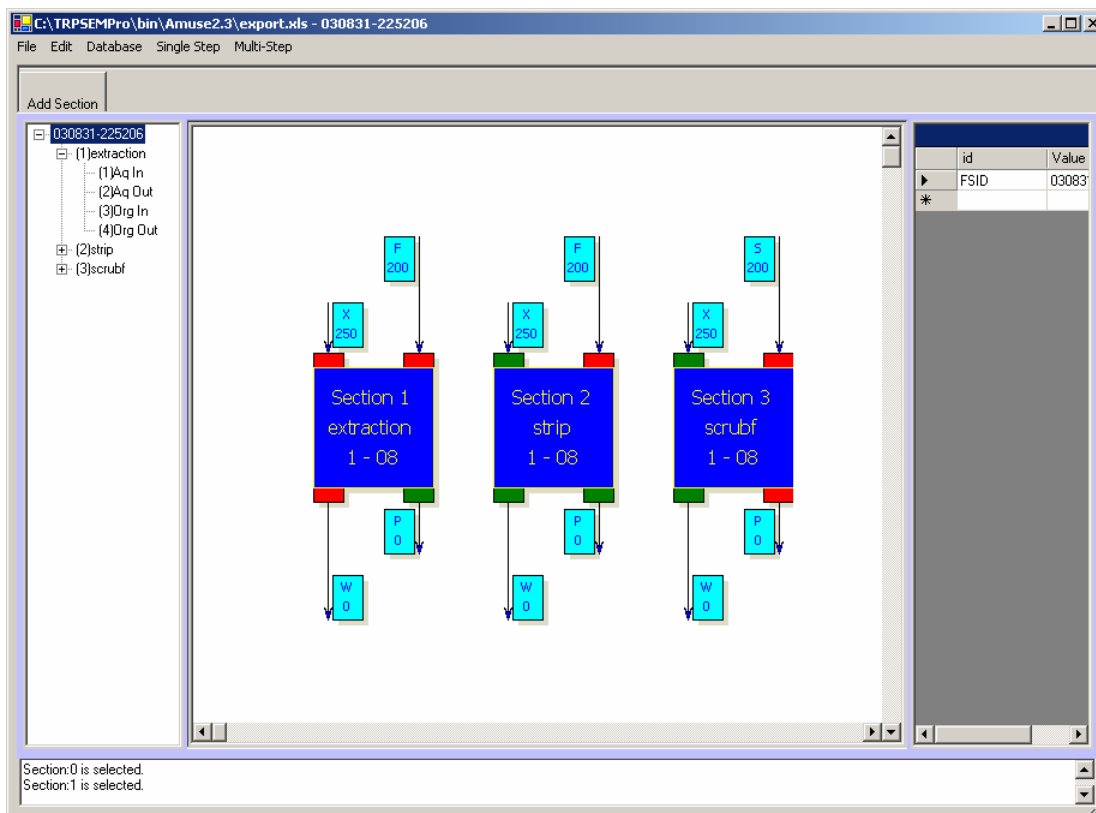


Figure 1.3.6. A FLOWSHEET-SIMULATOR screen

Task-Integration module has been continuously developed and revised to perform the following:

- Create a new task from scratch
- User can dynamically add simulation module, simulation code, and chemical separation module such as AMUSE code to the main task
- User can dynamically define the dataflow among all the tasks
- Save the simulation results to the developed database
- Save the simulation results as XML file

The Task-Integration module can be used to build the whole flowsheet to simulate the chemical separation process. User can then apply the different system study tools to study the system

engineering modeling and analysis from the Task-Manager module. The Task-Manager module has been designed. Currently, we are in the coding phase.

## TRANSMUTATION SCIENCES

**Niobium Cavity Fabrication Optimization (Task 2).** Multipacting is one of the major loss mechanisms in rf superconductivity cavities for accelerators. This loss mechanism limits the maximum amount of energy/power supported by the cavities. Optimal designs have been identified in others' studies. In practice, these designs are not easily manufactured. Chemical etching processes used to polish the cavity walls result in a nonuniform surface etch. A nonuniform surface etch will leave some unclean areas with contaminants and micron size particles. These significantly affect multipacting. Further, a nonuniform etch will leave areas with damaged grain structure, which is not good for superconducting properties. Typically, the depth of chemical polishing etch ranges between 10 to 150 microns.

Multipacting Studies: Possible multipacting scenarios were evaluated using the research code provided to us by Field Precision. Results do not appear to yield clear cut evidence of multipacting. One may deduce that multipacting might occur by examining the probability that a secondary electron is emitted from the surface of the material under test. In this case, one narrows in on those primary electrons exhibiting a large number of impacts. A primary electron yielding ten impacts may have a high enough probability of generating a couple of secondary electrons. Particles exhibiting a large numbers of impacts are sought. Once identified, their particle orbits are then examined to determine if they exhibit some periodic trajectory. This periodic motion is a sign of multipacting. Many of the particles exhibiting large numbers of orbits do exhibit this periodic motion but the probability of secondary emission is low on an impact. Further the particle orbit is usually terminated because the emitted charge does not have enough kinetic energy to overcome the binding energy of the surface of the niobium under test. The major difficulty that arises with the application of the code is repeatability. The random number generator internal to the code used as an aid in characterizing the surface and bulk physics of the medium inhibits repeatability.

Experimental Set-up for the Secondary Electron Emission from a Niobium Test Piece: Field and geometry requirements for a position sensitive MCP/RAE electron sensor, electron gun specifications, sample size and cryostat geometry, optimal locations and potentials were obtained to detect single secondary electrons emitted from a niobium sample with various energies and trajectories. For practical reasons, the geometry may be modified by placing a number of known bevels over the hemispherical surface. This will aid in eliminating alignment issues. With a proper grid potential, all secondary electrons can be collected. Upon completion of the study, an electron position detector, power system, grid, and electron gun were ordered. It is anticipated that the system will be installed in the vacuum chamber next quarter.

Experimental Visualization of the Verification of the Etching Process: When CFD results were presented to LANL personnel, they strongly recommended experimental flow visualization of etching process inside the cavity, to help verify FEA simulations and to get better insight into the problem. They also agreed to loan a transparent plastic cavity that will be used at UNLV to simulate etching conditions.

The cavity is supported by a plexiglass box, which is filled with water to reduce reflection. The baffle is placed inside the cavity. Fluid enters the inlet section of the cavity from the tank and exits to reach the bottom tank. Valves are used to control the flow inside the cavity to achieve the required flow rate.

Verification of the predicted velocity distributions in a prototype niobium cavity using acid etchant can be hazardous. Fortunately, laminar and turbulent flow distributions can be verified experimentally through dynamic similitude by choosing a fluid flow that has the same Reynolds number for the desired flow rate. By matching the Reynolds number of the flow in a model to the prototype cavity, the resulting flow patterns will be the same.

The CFD results indicated that the performance is better when the flow exit is axial to the flow inlet, but it is not practically feasible to create a larger single circular segment for flow exit as it removes the support for the baffle. Instead small circular holes are drilled to achieve the required condition. The effect of replacing the four holes arrangement instead of a single circular segment is also analyzed using CFD. Both the graphical plots and the numerical values show that four holes arrangement for exit can be substituted for a single circular segment without affecting the results.

Based on the drawings from LANL, a baffle was fabricated using plexiglass. It was then fixed into the cavity and analyzed for flow pattern. In the CFD results the streamlines with relatively high velocity values are concentrated in the region 0.08m from the centerline of the cavity, which corresponds to 0.03 from the baffle tip. This high velocity region in the experimental image is identified by band of streamlines, which displace the dye more rapidly, and occurs at a distance of 0.0224 from the baffle tip. This value is comparable to 0.03m in CFD model. Both results show less penetration inside the cavity cells, with more circulation only near the iris regions.

**Environment-induced Degradation of Materials (Task 4).** C-ring and U-bend specimens of Alloys HT-9 and EP-823 have been tested at 95 and 98% yield strength of these alloys at ambient temperature, 50 and 100°C in acidic solution using a Hasteloy C-276 autoclave. Testing at ambient temperature has been conducted with and without the presence of oxygen. Evaluation of the tested specimens for cracking is in progress using optical microscopy.

A significant number of SCC tests using calibrated proof rings, and smooth and notched tensile specimens of martensitic Type 422 stainless steel, and Alloys EP-823 and HT-9 has been completed in both neutral and acidic aqueous environments under constant-load conditions at ambient and elevated temperatures. In case of Type 422 stainless, the threshold stresses for notched and smooth specimens were determined. Additional tests are ongoing using Alloys HT-9 and EP-823 to determine their threshold stresses.

Metallographic and fractographic evaluations of all specimens tested under constant-load and slow-strain-rate conditions are in progress.

Localized corrosion studies using an electrochemical method are ongoing to evaluate the critical potentials in both neutral and acidic environments at elevated temperatures.

**LBE Corrosion Modeling (Task 5).** Runs were completed on simulating a 2-D sudden expansion geometry with certain imposed concentration values on the walls downstream from the expansion. This work is in preparation for the 3-D sudden expansion which will be started in the next phase of the project. Some grid independency tests were performed on laminar and turbulent flows in different geometries and perform several parametric runs of variations of  $Re$ ,  $Sc$ , oxygen concentration and other important quantities that affect the magnitude of corrosion/precipitation fluxes in a 3-D lead-bismuth flow loop. A new graduate student has joined the group and is working on the 3-D sudden expansion flow models amongst others.

The final check for the benchmarking process is to check for the dependency of the obtained results on the grid structure. Figure 1.3.7 shows the graph depicting the grid independency check. The procedure considers three different grid structures and running the model with the same boundary conditions. The corrosion/precipitation rate from all the three runs has been compared. It can be seen that the results do not vary by a lot with the change in grid structure. The percentage error in the 'fine' and 'finer' grids seems to be in better agreement than the 'coarse' grid. Hence it could be concluded that the results from the 'fine' grid structure are independent of mesh distribution.

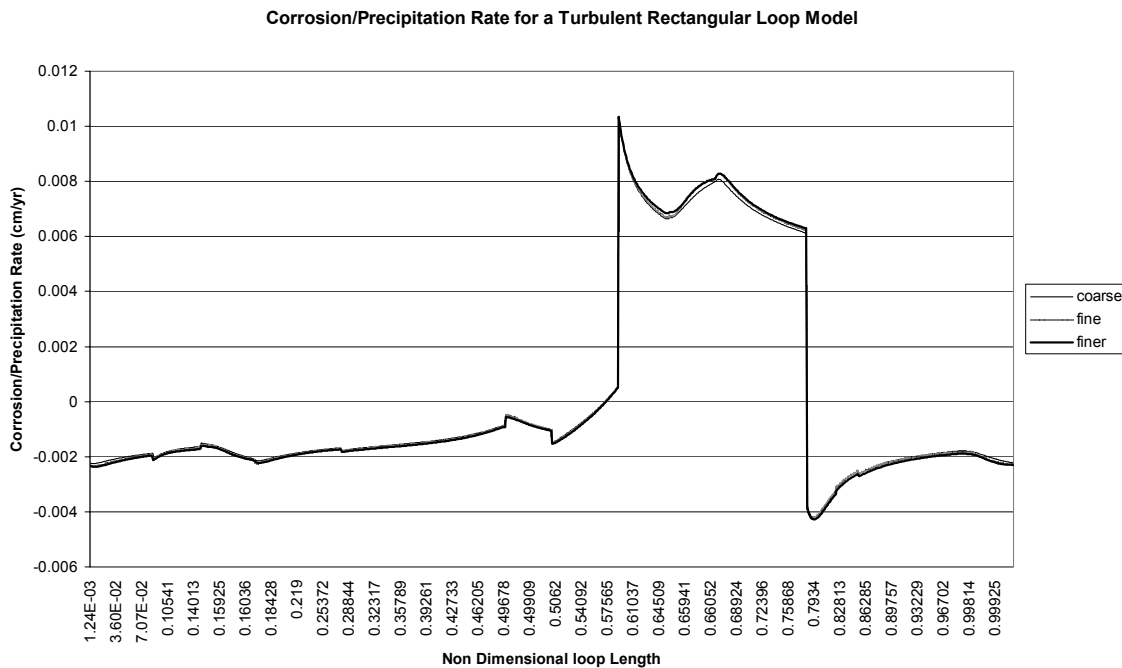


Figure 1.3.7. Grid Independency Check for a Turbulent Rectangular Loop Model

This study has shown that the simulation results are consistent with the analytical results and hence the process of benchmarking the CFD code is successful. The research has then been extended to further analyze the effect of various parameters on mass diffusion.

A parametric study has been carried out for the rectangular loop model with Reynolds number, Schmidt number, initial oxygen concentration and temperature variation along the loop length as

parameters. The studies have been carried out both in the laminar and turbulent regimes. The parametric studies are mainly useful in determining the most critical points in the Materials Test Loop (MTL) i.e. the points of maximal or minimal corrosion and helps decide on the most favorable parameters to run the loop with longest possible life.

**Properties of Alloy EP-823 (Task 10).** Temperature profiles have been developed to determine the times needed to achieve the desired test temperature, as a part of the furnace calibration process.

Testing has been performed at ambient temperature, 100<sup>0</sup>C and 300<sup>0</sup>C using tensile specimens fabricated from vacuum-melted and heat-treated (at the Timken Company, OH) bars of martensitic Alloy EP-823 (heat number 2054 and different tempering times). Preliminary data indicate that both the yield strength (YS) and the ultimate tensile strength (UTS) of the tested material were slightly reduced at the elevated temperatures. However, no significant reduction in ductility in terms of percent elongation (%El) and percent reduction in area (%RA) was observed in these tests.

Performed thermal treatments of Alloys EP-823 and HT-9 of different heats (2056 and 2048 respectively). Test specimens are being fabricated.

**Oxygen Sensing in LBE (Task 13).** Although liquid lead-bismuth eutectic (LBE) is a good candidate as a coolant in fast nuclear systems, it is known to be very corrosive to stainless steel, the material of the carrying tubes and containers. Such a corrosion problem can be prevented by producing and maintaining a protective oxide layer on the exposed surface of stainless steel. The proper formation of this oxide layer critically depends on the accurate measurement and control of the oxygen concentration in liquid LBE. YSZ (Yttria Stabilized Zirconia) oxygen sensors, using molten bismuth saturated with oxygen as the reference, have been utilized to accurately measure the concentration of oxygen dissolved in LBE. Two experimental setups have been assembled in LANL, one system is from UNLV and the other is from LANL. Some preliminary results regarding the simulations for the transport phenomena in the new apparatus have been obtained.

**Positron Annihilation Spectroscopy (Task 14).** The purpose of this collaborative research project involving UNLV, ISU, and LANL is to evaluate the feasibility of determining residual stresses in cold-worked, plastically-deformed (bent), and welded materials using a nondestructive method based on positron annihilation spectroscopy (PAS). This technique uses  $\gamma$ -rays from a small MeV electron Linac to generate positrons inside the sample via pair production. This method is known to have capabilities of characterizing defects in thick specimens that could not be accomplished by conventional positron technique or other nondestructive methods. The generated data will be compared to those obtained by other methods such as neutron diffraction and X-ray diffraction (for thin specimens), and ring-core (destructive-for thick specimens) methods.

A Linear Accelerator (Linac) of higher frequency was used to measure residual stresses using the PAS technique to perform the measurements more precisely. Measurements were performed on the cold-worked and the welded specimens of Type 304L Stainless Steel (SS) and Alloy EP-823.

A research proposal was submitted to the Atomic Energy of Canada Ltd (AECL) to perform residual stress measurements on different configurations of test specimens using the neutron diffraction technique.

A different research facility (Oakland University in Michigan) was identified to perform ring-core measurements on test specimens of different configurations.

A vacuum-induction-melt of Alloy HT-9 was prepared at the Timken Company for fabricating different kinds of test specimens for future residual stress measurements.